



# Velocity fluctuations inside two and three dimensional silos

Iker Zuriguel<sup>1</sup> · Diego Maza<sup>1</sup> · Alvaro Janda<sup>2</sup> · Raúl Cruz Hidalgo<sup>1</sup> · Angel Garcimartín<sup>1</sup>

Received: 4 February 2019  
© Springer-Verlag GmbH Germany, part of Springer Nature 2019

## Abstract

In this paper we report experimental and numerical results on the velocity fluctuations of grains inside silos. Although simple models exist for the stationary and continuous approximation of the flow, the variability at the microscopic level (both ensemble averages and the fluctuations of individual particles around the average) reveal non-Gaussian statistics that resist a straightforward treatment. We also show that decreasing the orifice size causes an increase in the relative amplitude of the velocity fluctuations, meaning that the intermittency grows bigger.

**Keywords** Silo · Hopper · Flow rate · Fluctuations

## 1 Introduction

Dense granular flows [1] are often approximated—especially in practical contexts—as continuous flows, for which average quantities (such as velocity or density fields) are deduced. It is therefore relevant to investigate how average values can be obtained from a system composed of grains where the nature of its intrinsic fluctuations is “athermal”. This topic has been considered in a wide range of systems [2], for instance, in a Couette geometry, where the fluctuating trajectories of the grain positions were used to obtain their diffusivity [3]. Nevertheless, when describing this system it is not always obvious how to define a temporal scale, a sort of threshold, above which particles behave diffusively (as in a Brownian random walker) instead of in a subdiffusive or superdiffusive fashion [4]. Accordingly, in order to develop continuous hydrodynamic approaches in granular flows [5], averaging must be performed over a length and a time scale that are hard to define [6].

Silos are often studied because of their industrial relevance [7, 8]. Although they display many typical features of

granular flows [9], silos may also include specific features such as clogging, imposed by geometrical restrictions near the outlet [10, 11]. Hence, if the orifice is not big enough, intermittent unstable flow interruptions [12, 13] notably affect the calculation of mean values. But even in the case where no interruption is observed (namely, for very large orifices) the fluctuations of the particles show nontrivial behavior [4, 14–16].

In this context, we lack a closed relationship that associates micromechanical features of the discharged material with the mass delivered through the silo outlet. About fifty years ago, Nedderman and Tüzün [17–19] proposed a straightforward kinematic model where the grain horizontal velocity  $u$  (or the radial one in the 3D case) would be proportional to the gradient of vertical velocity,  $v$ , along the horizontal direction  $x$ . Then  $u = -B \frac{\partial v}{\partial x}$  where  $B$  is a constant with length dimensions that the authors named a “kinematic” constant. Assuming that the granular material behaves as an incompressible fluid, the continuity equation allows to express the relationship between velocity components as a parabolic partial differential equation:

$$\frac{\partial v}{\partial z} = -B \frac{\partial^2 v}{\partial x^2} \quad (1)$$

where  $z$  accounts for the vertical coordinate.

As this expression resembles the 1D diffusion equation (where  $z$  replaces time), many authors tend to think of  $B$  as a diffusivity, or more specifically as a diffusion length. Although this idea seems reasonable, and coherent with previous diffusive approaches introduced by Litwiniszyn

---

This article is part of the Topical Collection: In Memoriam of Robert P. Behringer.

✉ Iker Zuriguel  
iker@unav.es

<sup>1</sup> Dpto. de Física y Mat. Apl., Fac. Ciencias, Universidad de Navarra, 31080 Pamplona, Spain

<sup>2</sup> Particle Analytics Ltd, Alrick Building, Max Born Crescent, The Kings Buildings, Edinburgh EH9 3BF, UK

and Mullins [20, 21], different experimental pieces of evidence showed that both approaches are at odds. Nevertheless, alternative stochastic explanations—where the plastic particle displacements are considered as a cooperative effect—provided a renewed interpretation of the relationship between  $B$  and a diffusion length [22, 23]. Leaving aside the microscopic interpretation of  $B$ , its value must be coherent with Eq. 1, which is usually solved applying the mass conservation principle and assuming that the lateral size of the container is much larger than the outlet size [17]. Under this condition, the volumetric flow rate,  $Q$ , at the silo outlet matches a delta function,  $Q(z=0) = Q\delta(x)$ , and the vertical velocity can be written as:

$$v = -\frac{Q}{\sqrt{4\pi Bz}} \exp\left(-\frac{x^2}{4Bz}\right) \quad (2)$$

If the flow is measured in grains per unit time, as we will do,  $Q$  must be divided by the number of grains per unit area. Note that the horizontal velocity can be obtained directly from Eqs. 1 and 2:

$$u = \frac{-Qx}{4\sqrt{\pi B}z^{\frac{3}{2}}} \exp\left(-\frac{x^2}{4Bz}\right) \quad (3)$$

In three dimensions,  $Q(z=0) = Q\delta(r)$  implies:

$$v = -\frac{Q}{4\pi Bz} \exp\left(-\frac{r^2}{4Bz}\right) \quad (4)$$

where we have used cylindrical coordinates,  $r$  being the distance to the cylinder axis. In this case if  $Q$  is measured in number of beads per unit time, it should be divided by the density of the packing (the density given in number of beads per volume).

In a previous work [24], we reported an analysis of the velocity of single grains in a two dimensional silo for a fixed orifice. We demonstrated that the average velocity profiles along the horizontal dimension were in good agreement with the theory put forward by Nedderman. Moreover, we demonstrated that the fluctuations of the vertical velocity at short time scales were close to a ballistic behaviour, whereas they seem to become diffusive at long time scales.

Recently, in a more extensive work, Thomas and Durian investigated the effect of the outlet size in the fluctuating grain dynamics [14]. In particular, a modification of the Kolmogorov Smirnov (KS) statistic was used to show that the intermittency grows as the outlet size reduces and increases the likelihood of clogging. Also, the relative velocity fluctuations and the skewness of the velocity distributions were proved to increase when the outlet was made smaller. Nevertheless, none of these parameters

displayed any evidence of the existence of a clogging transition for a given value of the outlet size.

In this work, we follow the same research line that in [14], extending the range of our previous observations [24] and exploring systematically the role that plays the outlet size on the kinematic model predictions. Importantly, our analysis covers exit widths where the flow is almost stationary and outlets where the flow is intermittent (and can eventually be arrested). In addition, we perform numerical simulations to check the validity of results obtained for a 2D experiment in a 3D cylindrical silo with a flat bottom having a circular orifice at the center.

The paper is organized as follows. In the next section, we will give a description of the experimental and numerical procedures. We will then provide the results for the velocity profiles of grains at different heights for different orifices. In the following sections we will describe long and short term velocity fluctuations. Finally, we will discuss their relevance and state some conclusions.

## 2 Materials and methods

We built a two dimensional silo made with two glass sheets that contains a monolayer of grains. In our setup, these spherical beads can be tracked and their velocity obtained with image processing techniques. Besides, we complement our experimental study performing simulations of a 3D cylindrical silo.

### 2.1 The experimental device

It consists of a large silo (800 mm high  $\times$  200 mm wide  $\times$  1.1 mm thick) filled with stainless steel monodisperse beads with a diameter  $d = 1.00 \pm 0.01$  mm that form a monolayer, albeit not strictly two-dimensional. The silo has an orifice at the bottom, whose width  $D$  has been varied within a range that covers the region where clogging is rather frequent ( $D < 5d$ ) and the region where, in practice, clogging would never occur ( $D > 7d$ ) [25–28]. In particular we have explored three orifice widths:  $D = 15.9, 9.7$  and  $4.8$  mm.

We recorded the beads with a high speed camera (Photron FASTCAM 1024 PCI). With a suitable optics, individual beads are distinguishable. A particle tracking software written at our laboratory was used to obtain the vertical velocities along a line spanning the whole silo width (200 mm) at several heights from the bottom (namely,  $z = 30, 65, 155$  and  $355$  mm). In order to analyze the fluctuations with greater spatio-temporal detail, we also tracked beads in smaller rectangular regions (20 bead diameter high  $\times$  5 bead diameters wide) centered along the vertical axis at the aforementioned heights. A thorough description of this experimental set-up

and a detailed explanation of experimental procedures can be found in [24].

## 2.2 Computer simulations

As grains inside three dimensional silos are not easily accessible, we have resorted to numerical simulations of a similar system. To this end, we used a hybrid CPU-GPU Discrete Element Model [29] algorithm which was previously shown to nicely reproduce the experimental findings in a 2D silo [30, 32]. We model a system of spherical glass particles with radius  $r_p = 3.0$  mm, that are initially placed at random positions in a flat bottomed cylindrical container. Spheres can leave the silo through a circular outlet of diameter  $D = 4.7$  and 6 (given in particle diameters) centered at the bottom. We use the Hertz contact model with nonlinear damping to compute the interaction force between contacting particles. In all the DEM calculations reported here the value of particle Young's modulus  $Y = 3.0 \times 10^9$  GPa, density  $\rho = 2650$  kg/m<sup>3</sup>, restitution coefficients  $e_n = e_t = 0.6$  and friction  $\mu = 0.5$  have been used.

## 3 Velocity profiles

In Fig. 1a, we plot both the horizontal  $u$  and vertical  $v$  bead velocities experimentally measured in a 2D silo with an orifice that is  $D = 9.7$  mm wide, at a height  $z = 65$  mm. From these data, we can directly check the basic conjecture of Nedderman and Tüzün. To this end, we fit Eq. 2 to  $v$ , leaving  $B$  and  $Q$  as free parameters, which is represented as a solid green line in Fig. 1a. We obtain  $B = 1.70$  mm and  $Q = 1875$  beads per second. The latter value is in excellent agreement with the one measured experimentally placing a scales at the bottom of the silo ( $Q = 1864$  beads per second). Aiming a further test of the robustness of this result, we fit the vertical velocity  $v$  using  $Q = 1864$ , and we obtain  $B = 1.69$  mm. In addition we can check the validity of Eq. 1 by inserting in Eq. 3 the  $B$  and  $Q$  values obtained from fitting the  $v$  profiles to Eq. 2. As shown in Fig. 1b, the agreement is remarkably good. For the horizontal component of the velocity, we can also fix  $Q = 1864$ , and then fit Eq. 3 to the experimental data. In this way, we obtain another value for  $B$  (1.57 mm) that we will call  $B'$  to indicate that it comes from fitting  $u$ . Note that in our procedure the origin  $x = 0$  is also left free because it may be a little bit displaced with respect to the silo axis (typically, about one particle diameter).

Once we have shown the agreement of the experimental data with Eqs. 2 and 3, in Fig. 2 we show the fits of  $v(x)$  corresponding to three orifice widths  $D = 15.9, 9.7$  and 4.8 mm obtained at different heights ( $z = 355, 155, 55$  and 30 mm) leaving free both  $B$  and  $Q$ . As the  $Q$  value obtained from the fits differ in less than 5% from the experimentally

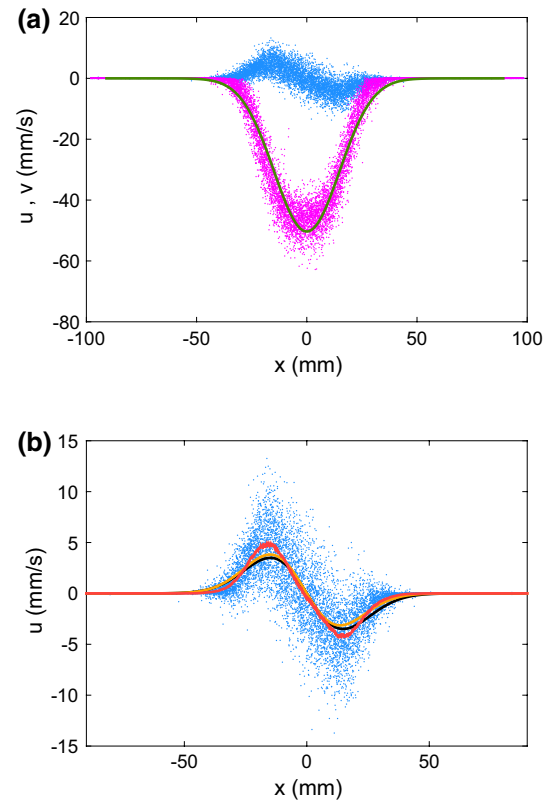


**Fig. 1** **a** Horizontal ( $u$ , blue) and vertical ( $v$ , magenta) experimentally measured velocities for  $D = 9.7$  mm and  $z = 65$  mm. The green solid line is the fit for Eq. 2, leaving  $B$  and  $Q$  as free parameters. **b** The horizontal velocity (same data than in a) with the smoothed experimental data (performed with a moving average, red solid line). The solid black line is the plot of Eq. 3 inserting the experimentally measured  $Q$  value and with  $B$  as obtained from the  $v$  fit in **a**. The orange solid line is a fit of Eq. 3 using the experimentally measured  $Q$  value and leaving  $B$  as the only free parameter. Note that just one tenth of the experimental data points, randomly chosen, have been represented to avoid cluttering the figure (colour figure online)

measured values of  $Q$ , we will use the latter in the following:  $Q = 4182, 1864$  and 555 beads per second for  $D = 15.9, 9.7$  and 4.8 mm, respectively. The values of  $B$  are provided in Table 1 for each case. Remark that  $B$  increases with height, a fact not predicted by the model which remains unexplained. In the same way, we implemented fits of  $u$  for all cases (not shown), obtaining the values of  $B'$  provided in Table 1. Let us note that in the case  $z = 355$  the error for  $B'$  may be quite big because the beads are moving slowly and across the whole silo width, so the fits for  $u$  are rather inaccurate. In all the other cases, the agreement between  $B$  and  $B'$  is quite good.

Computer simulations in three dimensions display a similar picture. In Fig. 3 we show the vertical velocities obtained in three-dimensional silos with a circular orifice at the base of diameter  $D = 4.7$  and 6  $d$  and four heights,  $z = 24, 20, 16$  and 12  $d$ , all values given in units

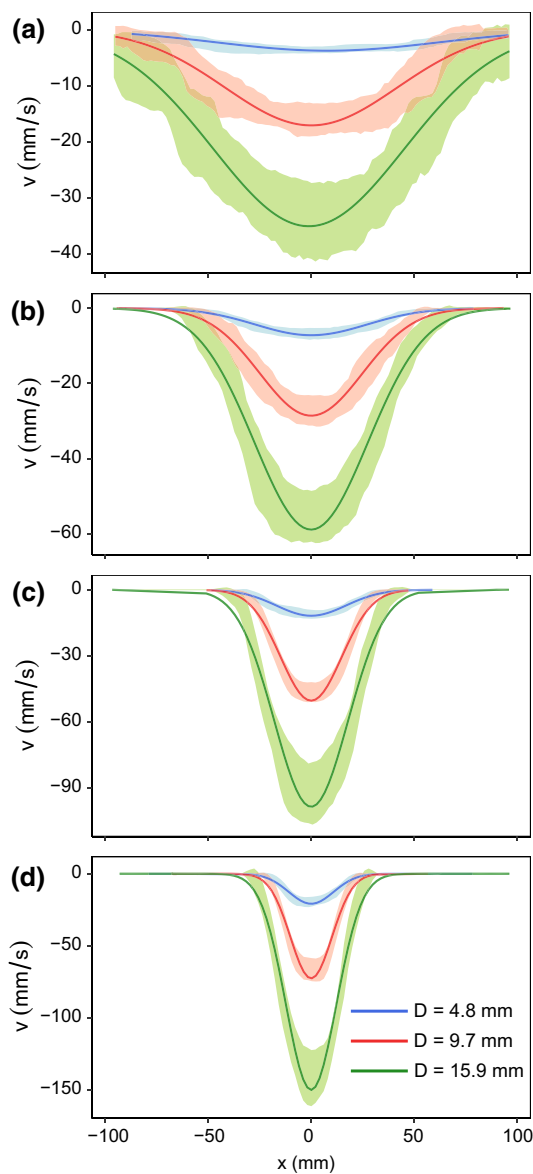


**Fig. 2** Profiles of the vertical velocity  $v(x)$  for different heights and different orifice sizes, as obtained experimentally in a two-dimensional silo. Note that the vertical scale is different for each plot. The heights are: **a**,  $z = 355$ ; **b**,  $z = 155$ ; **c**,  $z = 55$ ; and **d**,  $z = 30$  mm. Different colors correspond to different orifice sizes: *blue*,  $D = 4.8$ ; *red*,  $D = 9.7$ ; *green*,  $D = 15.9$  mm. The lines are fits for Eq. 2. The shadowed regions display a band of one standard deviation  $\sigma$  around the average velocity profile  $\langle v(x) \rangle$ . More than  $10^4$  individual measurements are included in each band (colour figure online)

of the particle diameter  $d = 2 \cdot r_p = 6$  mm. These velocities are an average over the azimuthal coordinate. At a height lower than 24, the mean velocity profiles agree with Gaussian curves, as in 2D experiments, and the values of  $B$  for Eq. 4 are given in Table 2. Note how  $B$  also increases with height. In the 3D silo, the mean velocity of grains at the top region of the silo is practically constant across the cross-section (data not shown), which is more

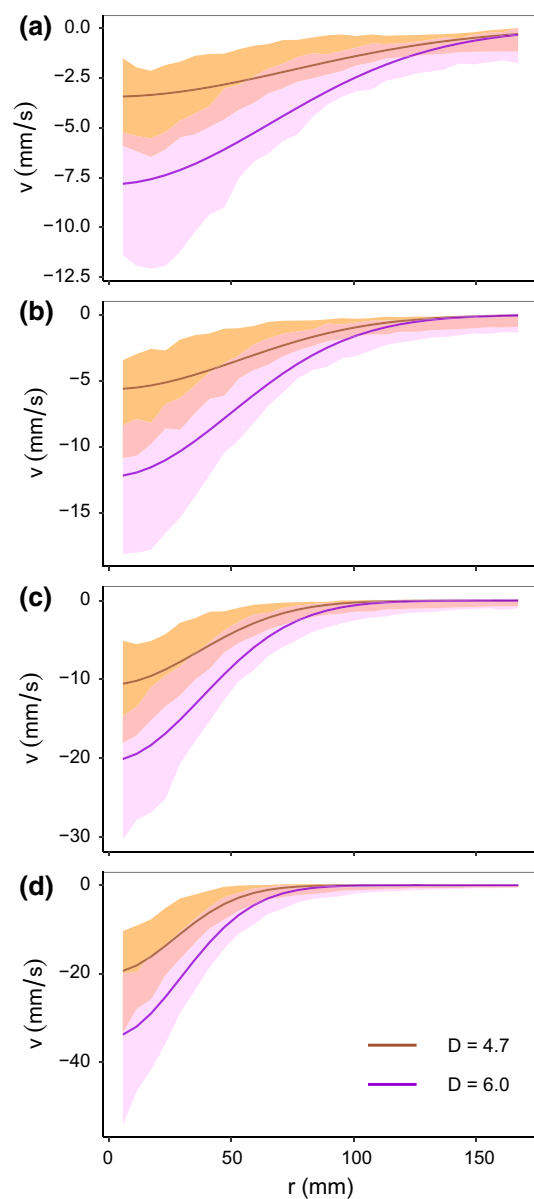


**Fig. 3** Profiles of the vertical velocity  $v(r)$  for different heights and different orifice size, as obtained in computer simulations of a cylindrical silo. Note that the vertical scale is different for each plot. The heights are: **a**  $z = 24$ ; **b**  $z = 20$ ; **c**  $z = 16$ ; and **d**  $z = 12$  (all in terms of the particle diameter,  $2r_p$ ). Different colours correspond to different orifice sizes: *brown*,  $D = 4.7$ ; *purple*  $D = 6$ . The lines are fits for Eq. 4. The shadowed regions display a band of one standard deviation  $\sigma$  around the average velocity profile  $\langle v(r) \rangle$ . More than  $10^5$  individual measurements are included in each band (colour figure online)

congruent with a plug flow. This result resembles the one that has been recently observed for soft frictionless spheres in 2D [31].

**Table 1** Values of the parameters obtained for the fit of experimental data to Eqs. 2 and 3

z (mm)	D (mm)	B (mm)	B' (mm)
355	15.9	3.14	1.91
355	9.7	2.59	2.69
355	4.8	4.74	2.98
155	15.9	2.54	2.39
155	9.7	2.12	1.94
155	4.8	2.78	2.13
65	15.9	2.33	2.10
65	9.7	1.69	1.57
65	4.8	2.51	1.77
30	15.9	2.23	2.18
30	9.7	1.72	1.54
30	4.8	1.91	1.76

B has been obtained from  $v$  and  $B'$  has been obtained from  $u$ .  $Q$  has been fixed to the experimentally measured values

**Table 2** Values of  $B$  obtained for the fit to Eq. 4, corresponding to the DEM simulations

z (mm)	D (mm)	B (mm)
24	6.0	2.50
24	4.7	2.63
20	6.0	1.97
20	4.7	1.99
16	6.0	1.50
16	4.7	1.35
12	6.0	1.16
12	4.7	0.96

The value of  $Q$  was measured for the two orifices of radius  $D = 6.0$  and  $4.7$ , giving  $Q = 1208$ , and  $573$  beads per second, respectively, and was inserted in the equation.  $D$  and  $B$  are given in terms of the particle diameter  $2r_p$

### 4 Velocity fluctuations

Remark that just displaying the velocities inside a confidence band from the average, as in Fig. 2, can be misleading, in the sense that important information is missing from this picture. In Fig. 4, for instance, experimental data corresponding to 20 different discharges for  $D = 9.7$  mm at  $z = 155$  mm have been collapsed into a single statistical ensemble assuming the ergodicity of the silo discharge process. One can detect two salient features. First, there are more deviations towards large downward velocities than on the other sense. And second, upon close inspection (see the arrow in Fig. 4a) “collective displacements”

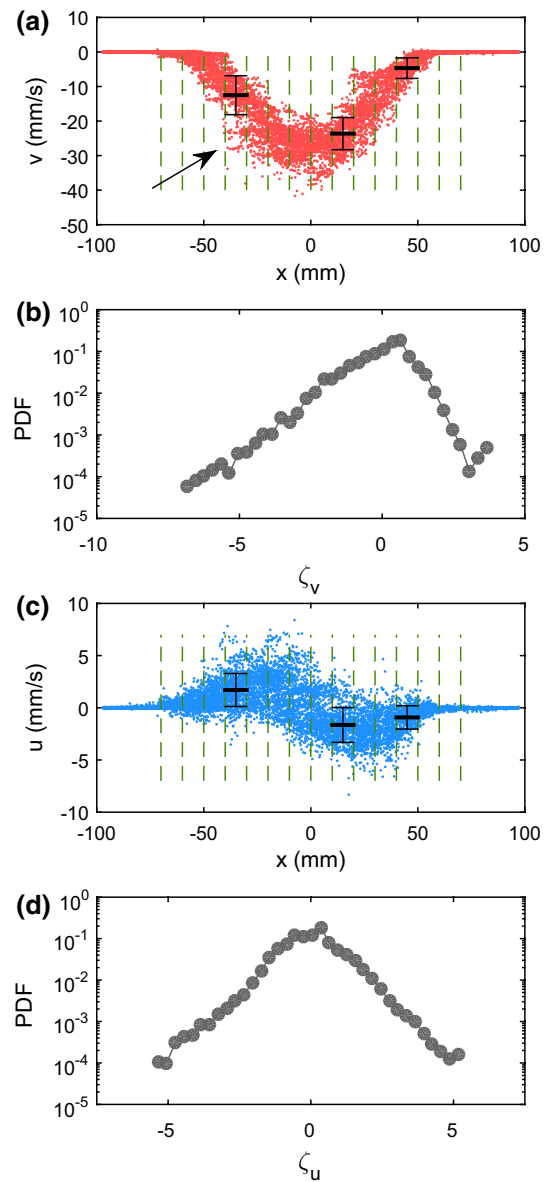


**Fig. 4** **a** Vertical velocities of grains, for  $D = 9.7$  mm at  $z = 155$  mm. Only 12,000 randomly selected data points are represented to avoid cluttering the figure (red dots). The data set has been split into 10 mm wide bands along  $x$ ; for each interval, the local average (thick solid lines) and  $\pm\sigma$  (thin solid lines) have been calculated (only a few are shown). The arrow marks a collective displacement. **b** The distribution of aggregated standardized vertical velocities  $\zeta_v$ . Remark that negative deviations correspond to larger downward speeds. **c** Horizontal velocity of grains for the same case than in **a** along with the mean and  $\pm\sigma$  bands (thick and thin solid lines; only a few are shown). **d** Standardized horizontal velocity distributions  $\zeta_u$ . Note that **b** and **d** are semilogarithmic plots (colour figure online)

(perceived as horizontal streaks at several parts of the graph) can be seen. These correspond to groups of beads falling together at almost the same speed in a solid-like fashion, or to put it more precisely, undergoing irreversible plastic deformations. Both features could be behind

the behavior of the mean average profile of  $v(x)$ , which is not perfectly Gaussian.

In order to further investigate this, we can take advantage of the large number of measurements we have. We analyze the velocities by considering several small intervals across the horizontal dimension of the silo (these are marked by dashed vertical lines in Fig. 4a). Inside each one of these intervals we have calculated the average  $v$ , that we call  $\langle v \rangle^x$ , and the  $\pm \sigma^x$  bounds around it, where the super-index  $x$  means that they are the *local* average and standard deviation for a given  $x$  interval. To the end of aggregating all the velocities together, we normalize  $v$  as  $\zeta_v = \frac{v - \langle v \rangle^x}{\sigma^x}$ .

Then all the  $\zeta_v$  values can be combined in a single distribution (Fig. 4b). Non-Gaussian fluctuations of the velocities around the mean are evident, so the behaviour is not diffusive. Also we corroborate that the distribution is biased towards large downward speeds. The picture emerging from computer simulations in three dimensions is not very different. In Fig. 5a the distribution of vertical velocities around the local mean are represented. The standardized fluctuations display long tails very similar to the 2D case, but the asymmetry is smaller. We hypothesize that this may be due to the reduced crystallization effects in 3D.

The same procedure can be carried out for horizontal velocities. In Fig. 4c we plot  $u$  (blue points), the average  $\langle u \rangle^x$  (thick solid black line), and the  $\pm \sigma^x$  bounds around it (thin solid black lines) for some intervals. We then take the deviations of  $u$  around the local mean and normalize  $u$  as before:  $\zeta_u = \frac{u - \langle u \rangle^x}{\sigma^x}$  (see Fig. 4d). In this case, fluctuations are approximately symmetrical, as gravity does not break the symmetry, but they lack a Gaussian shape. The same can be said of the 3D case (Fig. 5b).

We have just shown how the velocities of particles inside the whole silo are not distributed normally. In two dimensions this may be due to the high degree of order, as beads are not randomly arranged far from the orifice. Instead, they tend to pack in an hexagonal lattice and move collectively performing plastic deformations. Nevertheless, in three-dimensional simulations fluctuations are neither Gaussian and ordering effects, if present, should be much smaller. Moreover, even though these fluctuations are ensemble averages of different experimental sequences, the resulting long-tailed distributions indicate that non-Gaussian fluctuations must be present in each of the explored experimental sequences.

To explore this feature in deep, we take high resolution and high velocity recordings at the formerly mentioned heights just in a rectangular region ( $5 \times 20$  mm) centered along the  $z$ -axis of the silo during more than 3 s. Hence, hundreds of particles are tracked to calculate the mean instantaneous velocity of the particles within the rectangular regions. In Fig. 6a we show an example of this. The instantaneous mean value of the particle velocities

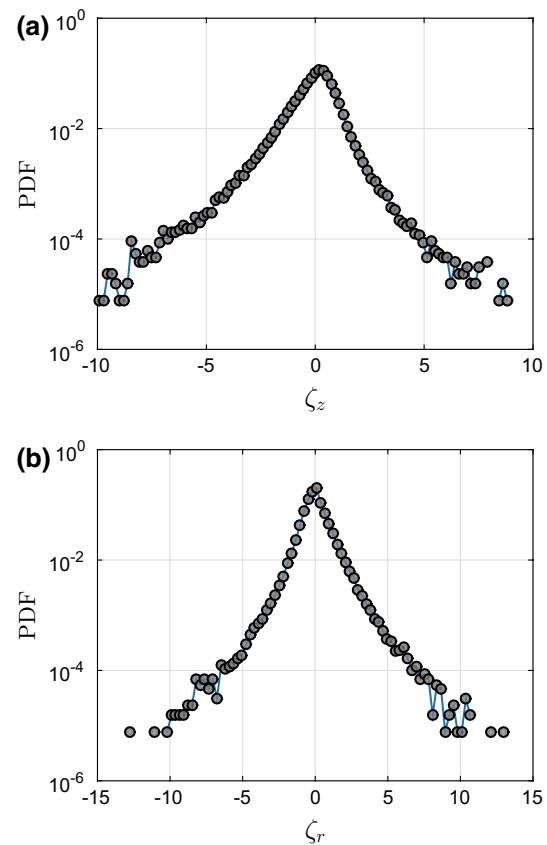


**Fig. 5** Distribution of the normalized velocities around the local mean obtained with DEM in a 3D silo for  $D = 4.7$  at  $z = 16$  (both given in terms of the particle size  $2r_p$ ); data correspond to the brown plot in Fig. 3c. **a** Standardized deviations  $\zeta_v$  of the vertical velocities. **b** Standardized deviations  $\zeta_p$  of the horizontal (radial) velocities

is displayed as a solid black line revealing that this is a strongly fluctuating magnitude with respect to its long term average  $v_c$ . Nevertheless, a high degree of correlation is also obvious when looking at the individual velocities (cyan lines): they all follow approximately the pattern of the instantaneous average velocity.

In order to analyze this behaviour we study the fluctuations of individual particle velocities with respect to the instantaneous mean value  $\langle v \rangle$  (Fig. 6b–e). Note that in this figure we have used the absolute value of  $v$ . Clearly, the larger the height, the smaller the range of the fluctuations. More importantly, it is also clear that for each  $z$ , the larger the outlet the larger the fluctuations. In order to compare the fluctuations corresponding to the three different outlet sizes, we have normalized them with respect  $v_c$  (Fig. 6f–i). Two relevant features become evident. The first one is that the long-tailed fluctuations—relative to the mean value—corresponding to small orifices (where clogging events are possible) are clearly more important than the ones appearing for large orifices. The second one is that near the outlet (Fig. 6e, i) long tailed fluctuations are still

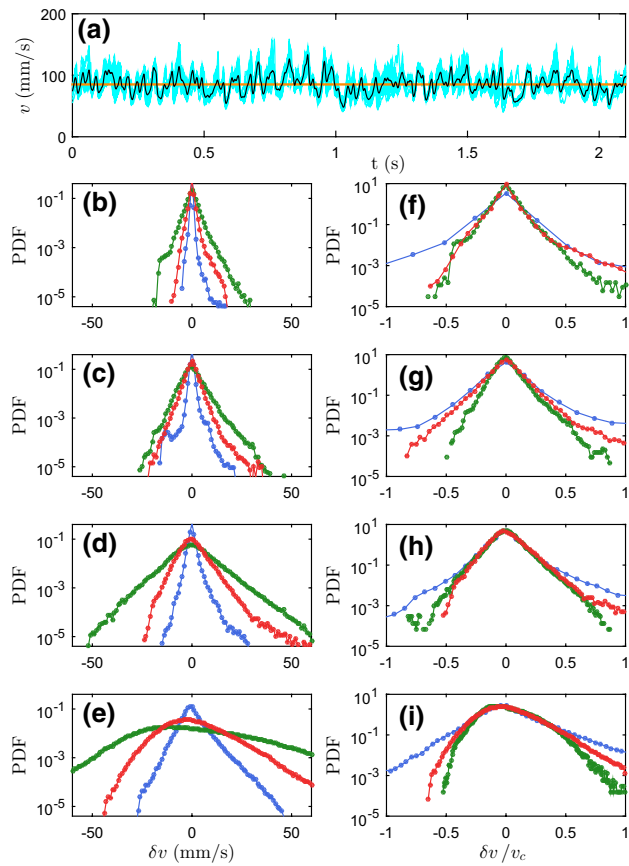


**Fig. 6** **a** The instantaneous vertical velocities for  $D = 15.9$  mm at  $z = 65$  mm. Remark that in this figure the module of  $v$  is used. Cyan lines are individual beads (only a few are shown) and the black solid line is the instantaneous average of all the beads  $\langle v \rangle$ . The horizontal orange line is the long time average value  $v_c$ . In the following panels the heights are: **b, f**  $z = 355$ ; **c, g**  $z = 155$ ; **d, h**  $z = 55$ ; and **e, i**  $z = 30$  mm. Different colors correspond to different orifice sizes: *blue*,  $D = 4.8$ ; *red*,  $D = 9.7$ ; *green*,  $D = 15.9$  mm. The distributions in the left column **b–e** are the variations of individual velocities  $\delta v$  with respect to the instantaneous average  $\langle v \rangle$ . The distributions in the right column **f–i** correspond to the said fluctuations with respect to  $\langle v \rangle$  rescaled by  $v_c$ . Note the semilogarithmic scales (colour figure online)

present for small orifices, but tend to become Gaussian for large orifices.

Similar features are also evident when analyzing the fluctuations of the instantaneous mean velocity  $\langle v \rangle$  around its long term average  $v_c$  (see Fig. 7). As before, the observed dynamics notably differs if small or large outlet apertures are considered. Now, the magnitude of the fluctuations are less pronounced and decay more rapidly. Moreover, the deviations from the Gaussian of  $\delta \langle v \rangle / v_c$  when far from the orifice are not as marked as before. Anyway, the tail towards larger (downward) velocities is heavier in all the cases analyzed.

Finally, we analyze the velocity fluctuations by looking at the variance of the vertical displacements

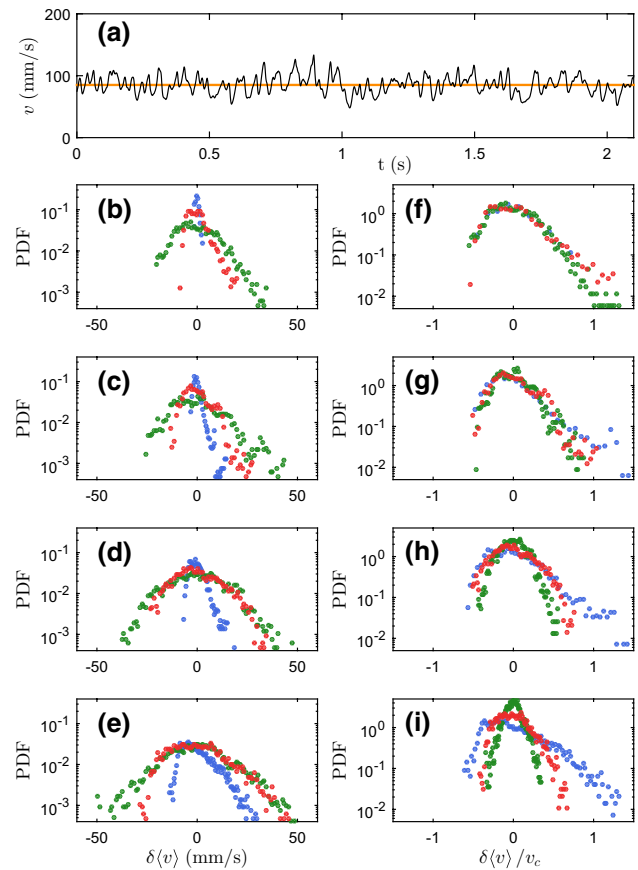


**Fig. 7** **a** The black solid line is the instantaneous average  $\langle v \rangle$  of all the beads  $D = 15.9$  at  $z = 65$  mm. Remark that in this figure the module of  $v$  is used. The orange horizontal line is the long time average  $v_c$ . In the following panels the heights are: **b, f**  $z = 355$ ; **c, g**  $z = 155$ ; **d, h**  $z = 55$ ; and **e, i**  $z = 30$  mm. Different colors correspond to different orifice sizes: *blue*,  $D = 4.8$ ; *red*,  $D = 9.7$ ; *green*,  $D = 15.9$  mm. The distributions in the left column **b–e** are the variations of the average  $\langle v \rangle$  with respect to  $v_c$ . The distributions in the right column **f–i** correspond to the said fluctuations rescaled by  $v_c$ . Note the semilogarithmic scales (colour figure online)

$\sigma^2 = \langle \Delta y^2 \rangle - \langle \Delta y \rangle^2$  and its dependence on the delay time  $t$  in which it is calculated. In Fig. 8 we report these measurements for different outlet sizes and silo heights. In all cases, we find that the fluctuations scale approximately as  $t^2$  for short times, indicating the existence of a ballistic regime which has been observed in many different granular dense flows [34, 35] including silos [14, 24]. The observation of this regime is also important from an experimental point of view as it guarantees that the sampling rate of the video recording is high enough to capture reliably the instantaneous velocity fluctuations [14]. As the delay time increases, the particles behave subdiffusively (the fluctuations scaling falls below  $\sigma^2 \sim t$ ) suggesting a cage effect [34, 35]. Unfortunately the experimental measurements were not long enough to assess whether the particles display

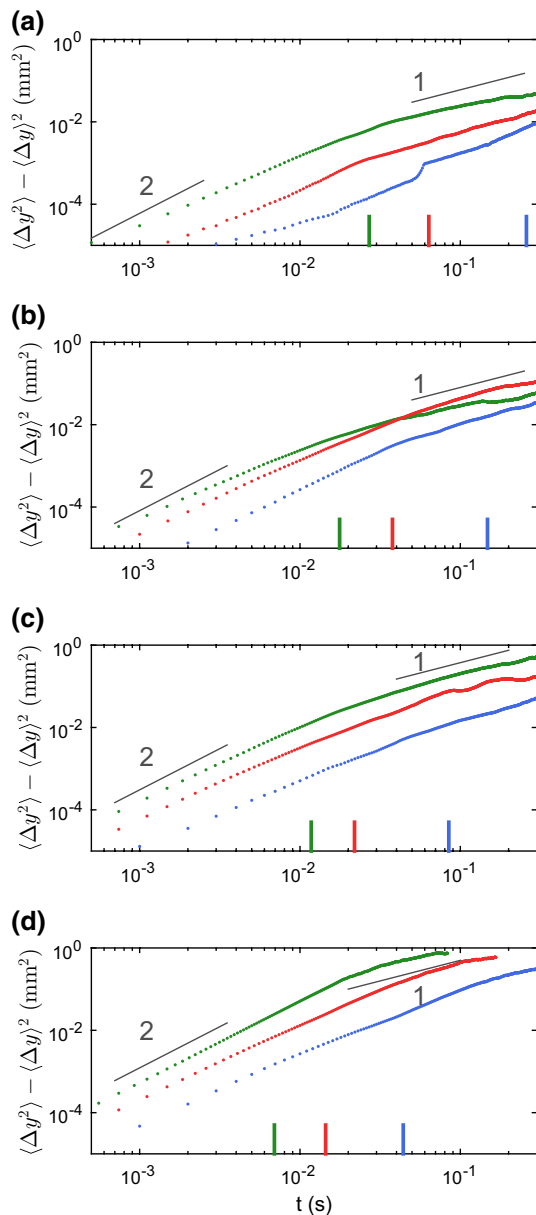


**Fig. 8** Variance of the particles displacements in the vertical direction at the four heights **a**  $y = 355$ , **b**  $y = 155$ , **c**  $y = 65$ , and **d**  $y = 30$  mm. Different colors correspond to different orifice sizes: *blue*,  $D = 4.8$ ; *red*,  $D = 9.7$ ; *green*,  $D = 15.9$  mm. Note that all the axes are at the same scale. The solid black lines are a guide for the eyes indicating a slope of 2 (ballistic regime), and a slope of 1 (diffusive regime). The vertical colored marks indicate (for each height and each outlet size) the average time that the particles need to travel a distance equal to its own diameter (colour figure online)

the expected diffusive motion for long delay times. Despite this experimental impediment, when comparing the different scenarios shown in Fig. 8, it can be guessed that the approximate time at which the curves start changing the slope reduces when increasing the outlet size and reducing the silo height. In principle, this correlates with the time that the particles take to travel its own diameter in each

case (indicated with different colours in Fig. 8) suggesting that this could be a good candidate for a characteristic time scale of the system.

## 5 Discussion

In this article we have shown how the particle velocity profiles in the silo discharge process still resist a straightforward interpretation. Despite the existence of some models that correlate the mean velocity profile with the microscopic dynamics, those models only agree partially with the observed experimental results. Indeed, although void diffusion moving through the discharging material is compatible with the existence of particle fluctuations, these fluctuations span along time scales larger than expected if some cage effect or diffusing spot model are assumed. The large spatio-temporal scales observed in the vertical velocity seem to be related to the propagation of plastic deformations through the bulk of the silo. Such plastic deformations could be related with the unstable arching process observed near the outlet, as reported in [30, 33].

We have also demonstrated how changing the orifice size affects the relative velocity fluctuations. The fluctuations of the vertical velocities  $v$  are always non Gaussian, and when rescaled by the long term average velocity  $v_c$ , they are larger for smaller orifices. The instantaneous average velocity  $\langle v \rangle$  can show fluctuations close to Gaussian far from the orifice, but near it the departure from that shape is more marked for small orifices.

We believe that the seminal ideas introduced by R.P. Behringer in his paper about self-diffusion in sheared granular media [2] and the subsequent extension [3] could be applied to the fluctuations driven by plastic deformation described in this work. We think that these articles will remain enlightening for future research.

**Acknowledgements** We acknowledge funding from Ministerio de Economía y Competitividad (Spanish Government) through Projects Nos. FIS2014-57325 and FIS2017-84631, MINECO/AEI/FEDER, UE. We would also like to express our gratitude to the late R. P. Behringer for all the discussions and talks we had with him, many of them concerning the topic of silo flow and clogging reported in this paper.

## Compliance with ethical standards

**Conflict of interest** We declare that we do not have any commercial or associative interest that represents a conflict of interest in connection with the work submitted.

## References

1. Duran, J.: Sands, Powders and Grains. Springer, New York (1999)
2. Behringer, R.P., Clément, E., Geng, J., Hartley, R., Howell, D., Reydellet, G., Utter, B.: Statistical properties of dense Granular



- matter. In: Hoogendoorn, S.P., Luding, S., Bovy, P.H.L., Schreckenberg, M., Wolf, D.E. (eds.) *Traffic and Granular Flow*, vol. 03, pp. 431–444. Springer, Berlin (2005)
3. Utter, B., Behringer, R.P.: Self-diffusion in dense granular shear flows. *Phys. Rev. E* **69**, 031308 (2004)
  4. Choi, J., Kudrolli, A., Rosales, R.R., Bazant, M.Z.: Diffusion and mixing in gravity-driven dense granular flows. *Phys. Rev. Lett.* **92**, 174301 (2004)
  5. Staron, L., Lagrée, P.-Y., Popinet, S.: Continuum simulation of the discharge of the granular silo. *Eur. Phys. J. E* **37**, 5 (2014)
  6. Jaeger, H.M., Nagel, S.R., Behringer, R.P.: Granular solids, liquids, and gases. *Rev. Mod. Phys.* **68**, 1259–1273 (1996)
  7. Jia, X., Gui, N., Yang, X., Tu, J., Jiang, S.: Experimental study and analysis of velocity correlation and intermittency of very slow and dense pebble flow in a silo bed. *Nuclear Eng. Des.* **305**, 626–638 (2016)
  8. Fullard, L.A., Davies, C.E., Neather, A.C., Breard, E.C.P., Godfrey, A.J.R., Lube, G.: Testing steady and transient velocity scalings in a silo. *Adv. Powder Technol.* **29**, 310–318 (2018)
  9. Medina, A., Córdova, J.A., Luna, E., Treviño, C.: Velocity field measurements in granular gravity flow in a near 2D silo. *Phys. Lett. A* **250**, 111–116 (1998)
  10. To, K., Lai, P.Y., Pak, H.K.: Jamming of granular flow in a two-dimensional hopper. *Phys. Rev. Lett.* **86**, 71 (2001)
  11. Zuriguel, I., Pugnaloni, L.A., Garcimartín, A., Maza, D.: Jamming during the discharge of grains from a silo described as a percolating transition. *Phys. Rev. E* **68**, 030301 (2003)
  12. Janda, A., Harich, R., Zuriguel, I., Maza, D., Cixous, P., Garcimartín, A.: Flow-rate fluctuations in the outpouring of grains from a two-dimensional silo. *Phys. Rev. E* **79**, 031302 (2009)
  13. Tewari, S., Dichter, M., Chakraborty, B.: Signatures of incipient jamming in collisional hopper flows. *Soft Matter* **9**, 5016–5024 (2013)
  14. Thomas, C.C., Durian, D.J.: Intermittency and velocity fluctuations in hopper flows prone to clogging. *Phys. Rev. E* **94**, 022901 (2016)
  15. Gardel, E., Seitaridou, E., Facto, K., Keene, E., Hattam, K., Easwar, N., Menon, N.: Dynamical fluctuations in dense granular flows. *Philos. Trans. R. Soc. A* **367**, 5109–5121 (2009)
  16. Szabó, B., Kovács, Z., Wegner, A., Ashour, A., Fischer, D., Stannarius, R., Börzsönyi, T.: Flow of anisometric particles in a quasi-two-dimensional hopper. *Phys. Rev. E* **97**, 062904 (2018)
  17. Nedderman, R.M.: *Statics and Kinematics of Granular Materials*. Cambridge University Press, Cambridge (1992)
  18. Nedderman, R.M., Tüzün, U.: A kinematic model for the flow of granular materials. *Powder Technol.* **22**, 243 (1979)
  19. Tüzün, U., Nedderman, R.M.: An investigation of the flow boundary during steady-state discharge from a funnel-flow bunker. *Powder Technol.* **31**, 27 (1982)
  20. Litwiniszyn, J.: The model of a random walk of particles adopted to researches on problem of mechanics of loose media. *Bull. Acad. Pol. Sci.* **11**, 593 (1963)
  21. Mullins, W.W.: Critique and comparison of two stochastic theories of gravity-induced particle flow. *Powder Technol.* **23**, 115 (1979)
  22. Kamrin, K., Bazant, M.Z.: Stochastic flow rule for granular materials. *Phys. Rev. E* **75**, 041301 (2007)
  23. Arévalo, R., Garcimartín, A., Maza, D.: Anomalous diffusion in silo drainage. *Eur. Phys. J. E* **23**, 191 (2007)
  24. Garcimartín, A., Zuriguel, I., Janda, A., Maza, D.: Fluctuations of grains inside a discharging two-dimensional silo. *Phys. Rev. E* **84**, 031309 (2011)
  25. Zuriguel, I., Garcimartín, A., Maza, D., Pugnaloni, L.A., Pastor, J.M.: Jamming during the discharge of granular matter from a silo. *Phys. Rev. E* **71**, 051303 (2005)
  26. Janda, A., Zuriguel, I., Garcimartín, A., Pugnaloni, L.A., Maza, D.: Jamming and critical outlet size in the discharge of a two-dimensional silo. *Europhys. Lett.* **84**, 44002 (2008)
  27. To, K.: Jamming transition in two-dimensional hoppers and silos. *Phys. Rev. E* **71**, 060301(R) (2005)
  28. Thomas, C.C., Durian, D.J.: Fraction of clogging configurations sampled by granular hopper flow. *Phys. Rev. Lett.* **114**, 178001 (2015)
  29. Hidalgo, R.C., Kanzaqui, T., Alonso-Marroquin, F., Luding, S.: On the use of graphics processing units (GPUs) for molecular dynamics simulation of spherical particles. *AIP Conf. Proc.* **1542**, 169–172 (2013)
  30. Rubio-Largo, S.M., Janda, A., Maza, D., Zuriguel, I., Hidalgo, R.C.: Disentangling the free-fall arch paradox in silo discharge. *Phys. Rev. Lett.* **114**, 238002 (2015)
  31. Ashour, A., Trittel, T., Börzsönyi, T., Stannarius, R.: Silo outflow of soft frictionless spheres. *Phys. Rev. Fluids* **2**, 123302 (2017)
  32. Hidalgo, R.C., Lozano, C., Zuriguel, I., Garcimartín, A.: Force analysis of clogging arches in a silo. *Gran. Matter* **15**, 841 (2013)
  33. Tang, J., Behringer, R.P.: How granular materials jam in a hopper. *Chaos* **21**, 041107 (2011)
  34. Menon, N., Durian, D.J.: Diffusing-wave spectroscopy of dynamics in a three-dimensional granular flow. *Science* **275**, 1920 (1997)
  35. Reis, P.M., Ingale, R.A., Shattuck, M.D.: Caging dynamics in a granular fluid. *Phys. Rev. Lett.* **98**, 188301 (2007)

**Publisher's Note** Springer Nature remains neutral with regard to jurisdictional claims in published maps and institutional affiliations.